

Article

Impact of Ionic Strength and Charge Density on Donnan Potential in the NaCl-Cation Exchange Membrane System

Baraa A. K. Al-Sakaji ¹, Ghaleb A. Hussein ² and Naif A. Darwish ^{2,*}¹ WS Atkins and Partners Overseas, Abu-Dhabi P.O. Box 7562, United Arab Emirates² Department of Chemical Engineering, American University of Sharjah, Sharjah 26666, United Arab Emirates; ghusseini@aus.edu

* Correspondence: ndarwish@aus.edu

Abstract: This work aims to theoretically investigate the effect of both the fixed charge density of ion exchange membranes and the ionic strength of the treated aqueous NaCl solution on the generated Donnan potential at thermodynamic equilibrium conditions. The direct objective of our work is to calculate the equilibrium concentration of the Cl⁻ co-ion inside a swelled cation-exchange membrane equilibrated with a water/NaCl system. Two activity coefficient models are employed, i.e., the Debye–Huckel (DH) model (as a reference model) and the Meissner model, which is known for its applicability in treating concentrated solutions. Experimental data available in the literature for Donnan potential are used to verify model predictions. Our study confirms that a high fixed charge density is required to counterbalance the deterioration in membrane selectivity encountered in high-salinity systems. The DH model can be safely used to predict the Donnan potential for feed compositions up to 0.1 M. At higher compositions, the DH model significantly overestimates the predicted (absolute) Donnan potential compared to the Meissner model. The osmotic pressure resulting from the difference in ionic concentration between the membrane phase and the feed phase is found to have insignificant effects on the Donnan potential. The equilibrium computations and methodology are presented in a general way that enables handling multivalent electrolyte systems such as CaCl₂.

Keywords: Donnan potential; ion-exchange membranes; the Meissner model; the Debye–Huckel model



Citation: Al-Sakaji, B.A.K.; Hussein, G.A.; Darwish, N.A. Impact of Ionic Strength and Charge Density on Donnan Potential in the NaCl-Cation Exchange Membrane System. *Water* **2023**, *15*, 3830. <https://doi.org/10.3390/w15213830>

Academic Editor: Licínio M. Gando-Ferreira

Received: 15 July 2023

Revised: 6 September 2023

Accepted: 26 September 2023

Published: 2 November 2023



Copyright: © 2023 by the authors. Licensee MDPI, Basel, Switzerland. This article is an open access article distributed under the terms and conditions of the Creative Commons Attribution (CC BY) license (<https://creativecommons.org/licenses/by/4.0/>).

1. Introduction

Ion-exchange membranes (IEMs) are vital in electrically driven membrane processes. They are used in a number of membrane-based separation processes, such as electrodialysis and electrochemical desalination [1–3]. In IEMs, stationary charged functional groups are attached to the polymer backbone of the polymeric membrane material. Ions of the same charge (i.e., co-ions) are completely or partially excluded from passing through the membrane. In contrast, ions of the opposite charge (i.e., counter-ions) are able to pass. Therefore, anion-exchange membranes have positively charged groups fixed to their polymeric skeleton and exclude positive ions (cations) but are freely permeable to negatively charged ions (anions). Similarly, cation exchange membranes with fixed negatively charged groups exclude anions but are freely permeable to cations. Electrical neutrality must be satisfied in all of these phenomena.

Industrial applications of ion-exchange membranes emerged more than half a century ago. Several IEM-based technologies have reached a satisfactory level of maturity that has advanced their utility to the large-scale commercial phase. For example, electrodialysis is now an essential technology in the brackish water desalination industry [4]. IEM found practical applications in many fields, such as the demineralization of industrial waste and whey and sugar liquor [5] and the purification of amino acid solutions [6]. Additionally, IEMs are utilized in several recent technologies, including electrodialysis reversal [7], bipolar membrane electrodialysis [8], electro-deionization [9], electrolysis [10], and diffusion

dialysis [11]. Yoshinobu Tanaka [12] authored an excellent book that addresses both the fundamentals and applications of IEMs.

When an IEM is equilibrated with a saline aqueous phase (including Na^+ , Mg^{+2} , Cl^- , etc.), an unequal distribution of ions arises between the hydrated (swelled) membrane and the aqueous phase, resulting in a phenomenon known as the Donnan electrical potential at the membrane/solution interface [13]. The Donnan potential results in a partial (or ideally a complete) exclusion of co-ions, providing the basis for the permselectivity of IEMs. Experimental measurement of the Donnan potential is expected to give important insight into the IEM's effective charge density, as the Donnan potential is strongly linked to the IEM charge density.

Despite the recent attempts to experimentally measure individual IEM-interphase Donnan's potentials, it is generally acknowledged that such measurements are extremely difficult [14]. Approximate methods based on measuring the overall potential difference in Donnan dialysis experiments were used in the past to predict the individual membrane-interphase Donnan potential [15]. Therefore, well-established theoretical methods to estimate the Donnan potential are usually employed [15–18].

In modeling the performance of IEMs, the treated aqueous phase (e.g., seawater) is usually assumed to be either an ideal solution, where values of the ionic activity coefficients become equal to one, or a real solution with equal ionic activity coefficients in both, the membrane and solution phases. In both cases, ion activity coefficients in the membrane and solution phases are eliminated from the analysis; the activities of the ions in both phases are replaced by their corresponding concentrations.

This work investigates the effect of the ionic strength of the treated solution and the fixed charge density of the IEM on the Donnan potential and IEM permselectivity at thermodynamic equilibrium conditions. Specifically, the co-ion concentration inside the IEM will be computed for different values of the treated solution compositions and the IEM fixed charge values. This study will employ the Debye–Huckel (DH) and Meissner corresponding state models to examine the Donnan electrochemical potential at the membrane/solution interface, which is assumed to be in thermodynamic equilibrium. The DH model, used here as a reference model, is rigorous and becomes exact at the infinite dilution limit of the electrolyte concentration. As such, it provides an anchor asymptotic framework for all other models of non-ideal systems. On the other hand, the Meissner corresponding state model, although an old model, is of high simplicity and applicability for highly concentrated aqueous solutions with molalities exceeding saturation [19]. Despite this, the model was not adequately addressed in the technical literature. In terms of the ionic mean activity coefficients (γ_{\pm}), the model showed excellent predictive capability [19]. Therefore, this “somewhat ignored” model will be used to compute the Donnan potential associated with an IEM equilibrated with an aqueous system of monovalent electrolyte, i.e., sodium chloride (NaCl). Specifically, the electrolyte mean activity coefficient in both phases, the aqueous feed and the swelled membrane, will be evaluated using the Meissner model, thus providing uniformity in calculating liquid phase nonideality. Experimental data for Donnan's potential of IEMs available in the literature will be used to verify the model's theoretical prediction.

2. Theory

2.1. The Donnan Equilibrium Theory

Consider a cationic exchange membrane in equilibrium with a saline aqueous phase (with ions like Na^+ , K^+ , Mg^{+2} , Ca^{+2} , Cl^- , OH^- , CO_3^{-2} , etc.). The chemical potential of each distributed ion (μ_i) in the swelled membrane phase (m) and the aqueous phase (s) is given as:

$$\mu_i^s = \mu_i^o(T, p^o) + RT \ln a_i^s + z_i \mathcal{F} \psi^s + \bar{V}_i^s (p^s - p^o) \quad (1)$$

$$\mu_i^m = \mu_i^o(T, p^o) + RT \ln a_i^m + z_i \mathcal{F} \psi^m + \bar{V}_i^m (p^m - p^o) \quad (2)$$

where μ_i^o is a reference chemical potential of species (i) at the system temperature (T) and a specified reference pressure (p^o), a_i is the activity of species (i), and z_i is the valence number of ion (i). Additionally, ψ is the electrical potential, \mathcal{F} is Faraday constant (96,500 C/mole), p is the pressure, and \bar{V}_i is partial molar volume of species (i). Superscripts (s) and (m) refer to the solution (feed) phase and the membrane phase, respectively. The last term in each of Equations (1) and (2) is usually neglected based on its very small contribution [13], and it will be neglected initially in our analysis here. However, the effect of their inclusion will be discussed separately in the next section.

At equilibrium, equality of the chemical potential of each ion requires that:

$$\mu_i^s = \mu_i^m \tag{3}$$

Substituting for μ_i^s and μ_i^m using Equations (1) and (2) (neglecting the last term in each) gives:

$$\frac{a_i^s}{a_i^m} = \exp\left(\frac{z_i \mathcal{F} (\psi^m - \psi^s)}{RT}\right) \tag{4}$$

The Donnan electric potential (E_{Don}) is $(\psi^m - \psi^s)$. Therefore, using Equation (4), we obtain the following:

$$E_{Don} = \frac{RT}{z_i \mathcal{F}} \ln\left(\frac{a_i^s}{a_i^m}\right) = \frac{RT}{z_i \mathcal{F}} \ln\left(\frac{C_i^s \gamma_i^s}{C_i^m \gamma_i^m}\right) \tag{5}$$

C_i stands for the concentration of ions (i), and γ_i is the activity coefficient of species (i). For a general salt $C_{\nu_C} A_{\nu_A}$ (e.g., CaCl_2) that ionizes completely:



where ν_C and ν_A stand for the stoichiometric numbers of the cation (C) and the anion (A) in the electrolyte $C_{\nu_C} A_{\nu_A}$. Writing Equation (4) for the cation and the anion and eliminating $\mathcal{F}(\psi^m - \psi^s)/RT$ between the two equations gives (with $a_i = C_i \gamma_i$):

$$(C_C^s \gamma_C^s)^{1/z_C} (C_A^s \gamma_A^s)^{-1/z_A} = (C_C^m \gamma_C^m)^{1/z_C} (C_A^m \gamma_A^m)^{-1/z_A} \tag{7}$$

The equations representing electrical neutrality for the membrane and the external solution are:

$$z_C C_C^m + z_A C_A^m - q = 0 \tag{8}$$

$$z_C C_C^s + z_A C_A^s = 0 \tag{9}$$

In Equation (8), q stands for the fixed charge density of the membrane in eq/liter. Equation (7), together with the electrical neutrality conditions for the membrane (Equation (8)) and the aqueous phase (Equation (9)), can be solved for the anion and cation concentrations inside the membrane and the Donnan potential as per Equation (5).

Substituting for C_C^m from Equation (8) and for C_C^s from Equation (9) into Equation (7) gives:

$$(-z_A/z_C)^{1/z_C} (C_A^s)^{1/z_C - 1/z_A} (\gamma_C^s)^{1/z_C} (\gamma_A^s)^{-1/z_A} = (\gamma_C^m)^{1/z_C} (\gamma_A^m)^{-1/z_A} \left(\frac{q - z_A C_A^m}{z_C}\right)^{1/z_C} (C_A^m)^{-1/z_A} \tag{10}$$

In the case of a (1–1) electrolyte (e.g., NaCl), $z_C = +1$ and $z_A = -1$, and for the case of a (2–1) electrolyte (e.g., CaCl_2), $z_C = +2$ and $z_A = -1$, Equation (10) gives:

$$\left(\frac{C_A^s}{C_A^m}\right) = \left(\frac{\gamma_{\pm}^m}{\gamma_{\pm}^s}\right) \left(\frac{q}{C_A^m} + 1\right)^{1/2} \quad (1-1) \text{ electrolyte} \tag{11}$$

$$\left(\frac{C_A^s}{C_A^m}\right) = \left(\frac{\gamma_{\pm}^m}{\gamma_{\pm}^s}\right) \left(\frac{q}{C_A^m} + 1\right)^{1/3} \quad (2-1) \text{ electrolyte} \quad (12)$$

$$\gamma_{\pm} = (\gamma_C^{v_C} \gamma_A^{v_A})^{\frac{1}{v_C+v_A}} \quad (13)$$

The mean activity coefficients in the membrane and aqueous phases γ_{\pm}^s are functions of the phase composition and temperature. These are calculated using specific liquid-phase models. In this work, the Debye–Huckel and Meissner models are used.

2.2. Effect of Osmotic Pressure on Donnan’s Potential

As shown in Section 2.1 above, the last term in Equations (1) and (2) is usually neglected based on its very small contribution [13]. Neglecting this term is essentially equivalent to neglecting the coupling between ion concentrations and the osmotic pressure. Julian et al. [20] pointed out that neglecting osmotic pressure effects and considering only ionic equilibrium may lead to an incorrect Donnan potential with an error dependent on the osmotic pressure. Gang Chen [21] also addressed the same issue and indicated that the existing coupling between ion concentrations and the osmotic pressure leads to a membrane potential that consists of not only the classical Donnan potential term but also an additional term due to the osmotic pressure. This implies the existence of a membrane potential even when the impermeable species are not charged.

In order to take into account the effect of the osmotic pressure on Donnan potential, the steps implemented above, shown in Equations (1) through (12), are employed again, but the last term in each of Equations (1) and (2) is not neglected. The procedure followed is the same as that mentioned in [20,21]. The equivalents of Equations (5), (11) and (12) when the pressure term is included are, respectively:

$$E_{Don} = \frac{RT}{z_i \mathcal{F}} \ln\left(\frac{a_i^s}{a_i^m}\right) - \frac{\pi \bar{V}_i}{z_i \mathcal{F}} = \frac{RT}{z_i \mathcal{F}} \ln\left(\frac{C_i^s \gamma_i^s}{C_i^m \gamma_i^m}\right) - \frac{\pi \bar{V}_i}{z_i \mathcal{F}} \quad (14)$$

$$\left(\frac{C_A^s}{C_A^m}\right) = \left(\frac{\gamma_{\pm}^m}{C \gamma_{\pm}^s}\right) \left(\frac{q}{C_A^m} + 1\right)^{\frac{1}{2}} f(\pi) \quad \text{with } f(\pi) = \exp\left(\frac{\pi \bar{V}_{solute}}{2RT}\right) \quad (1-1) \text{ electrolyte} \quad (15)$$

$$\left(\frac{C_A^s}{C_A^m}\right) = \left(\frac{\gamma_{\pm}^m}{C \gamma_{\pm}^s}\right) \left(\frac{q}{C_A^m} + 1\right)^{\frac{1}{2}} g(\pi) \quad \text{with } g(\pi) = \exp\left(\frac{\pi \bar{V}_{solute}}{3RT}\right) \quad (2-1) \text{ electrolyte} \quad (16)$$

where π stands for the osmotic pressure difference across the membrane ($p^m - p^s$), which arises because of the electrolyte concentration difference between the swelled membrane phase and the feed phase.

It is to be noted that the osmotic pressure π depends on the electrolyte concentration in both phases, including C_A^m , which is the unknown variable in Equations (15) and (16). The functional dependence of π on C_A^m and C_A^s is obtained by implementing the equilibrium criterion for the solvent (water) by equating the chemical potential of water in the swelled membrane phase and the feed phase ($\mu_{water}^m = \mu_{water}^s$). This results in the following expression for π :

$$\pi = \frac{RT}{\bar{V}_{water}} \ln \frac{a_{water}^s}{a_{water}^m} = \frac{RT}{\bar{V}_{water}} \ln \frac{x_{water}^s \gamma_{water}^s}{x_{water}^m \gamma_{water}^m} \quad (17)$$

Substituting for π from Equation (17) into Equations (15) and (16) for $f(\pi)$ and $g(\pi)$ gives:

$$f(\pi) = \exp\left(\frac{\bar{V}_{solute}}{2RT} \frac{RT}{\bar{V}_{water}} \ln \frac{a_{water}^s}{a_{water}^m}\right) = \left(\frac{a_{water}^s}{a_{water}^m}\right)^{\frac{\bar{V}_{solute}}{2\bar{V}_{water}}} \quad (1-1) \text{ electrolyte} \quad (18)$$

$$g(\pi) = \exp\left(\frac{\bar{V}_{solute}}{3RT} \frac{RT}{\bar{V}_{water}} \ln \frac{a_{water}^s}{a_{water}^m}\right) = \left(\frac{a_{water}^s}{a_{water}^m}\right)^{\frac{\bar{V}_{solute}}{3\bar{V}_{water}}} (2-1) \text{ electrolyte} \quad (19)$$

In the Results and Discussion section, we will show that under the prevailing conditions of the membrane fixed charge density and the external solution concentration, there is practically no effect for $f(\pi)$ and $g(\pi)$, i.e., both have an approximate value of unity.

2.3. The Debye–Huckel Theory

According to this theory, the nonideality of an electrolyte solution is expressed as the sum of the separate contributions of coulombic forces from solvent-ion and ion-ion interactions. These contributions fundamentally differ from the dispersive van der Waals forces acting between neutral molecules. The DH theory provides an exact model for the mean activity coefficient (γ_{\pm}) at the electrolyte infinite dilution limit. Thus, it stands as a rigorous anchor point for most engineering models of electrolyte solutions. Debye–Huckel theory incorporates several key simplifications [21]: (1) the solvent is a structureless continuum with constant permittivity (ϵ) and dielectric strength (D_s); (2) the ions are spherically symmetric; and (3) the charge density around each specified ion is obeying a continuous Poisson–Boltzmann distribution.

The derivation of a mathematical model for the mean electrolyte activity coefficient (γ_{\pm}), which is based on the DH theory, can be phenomenological and based on the concepts of classical electrostatics [21]. It can also be derived based on the concepts of statistical mechanics [22]. The phenomenological approach gives the following mathematical expression for the mean activity coefficient (γ_{\pm}) of an electrolyte in a solution:

$$\log_{10} \gamma_{\pm} = \left(\frac{1.8248 \times 10^6 \rho_s^{1/2}}{(D_s T)^{3/2}}\right) (z_C z_A) I^{1/2} \quad (20)$$

$$I = \frac{1}{2} \sum_i m_i z_i^2 \quad (21)$$

where I is the ionic strength of the solution, m_i is the molality of species (i) (mole i/kg solvent), which becomes approximately c_i (mole i/L solvent) for dilute solutions, ρ_s is the solvent density, and D_s is the dielectric constant for the solvent.

2.4. The Meissner Corresponding State Model

The DH model gets progressively worse as ionic strength increases beyond 0.01. The non-ideal behavior of electrolyte solutions, expressed in terms of the electrolyte mean activity coefficient γ_{\pm} , generally shows a very complex functional relationship with concentrations and temperature. Ideally, a robust theoretical model that predicts this complex functional relationship becomes a necessity. One example of such robust models, which was not adequately emphasized in the technical literature, is the Meissner corresponding state model.

Meissner and Tester [23] recognized a possible similar approach to generalize the non-ideal mean ionic activity coefficient (γ_{\pm}) behavior of strong electrolytes. They were inspired by the great success of the law of the corresponding states in correlating the PVTN behavior of gases and liquids. The developed generalized model ably captured the very complex nature of the functional dependence of γ_{\pm} on electrolyte concentration and electrolyte chemical nature. For example, some electrolytes like HCl and LiCl show strong positive deviations ($\gamma_{\pm} > 1$), while others like CuSO₄ show negative deviations ($\gamma_{\pm} < 1$). The model maintains consistency with the DH at the infinite dilution limit of the electrolyte, i.e., $\gamma_{\pm} = 1$ as $m = 0$. Specifically, the reduced activity coefficient ($\Gamma_{ij}^o \equiv \gamma_{\pm}^{\frac{1}{|z_C z_A|}}$) was found to provide a limiting result that was independent of electrolyte type. Meissner and Tester [23] explored the idea of using Γ_{ij}^o outside the DH region to correlate pure single

electrolyte γ_{\pm} data for over 120 different electrolytes. It was found that $\log_{10}\Gamma_{ij}^o$ versus I formed a family of non-intersecting curves quite analogous to the compressibility factor chart ($Z = f(T_r, P_r; \omega)$). What is remarkable about this model is its extrapolative nature to significantly higher concentrations, even up to ionic strengths of 20 or more [19]. Further refinements by Meissner and others produced the final generalized correlation of the model, as follows [23]:

$$\begin{aligned} \gamma_{\pm}^{1/|z_c z_a|} &= \left[1 + B(1 + 0.1 I)q_{ij}^o - B \right] \Gamma_{ij}^{DH} \\ \log_{10}\Gamma_{ij}^{DH} &= \frac{-0.5107I^{1/2}}{1+CI^{1/2}} \\ B &= 0.75 - 0.065q_{ij}^o; C = 1 + 0.055q_{ij}^o \exp(-0.023I^3) \end{aligned} \quad (22)$$

The parameter q_{ij}^o was reported for many electrolytes at 25 °C and was extrapolated to other temperatures using the following formula:

$$q_{ij}^o(T) = q_{ij}^o(T_{ref}) \left(1 - \frac{0.0027(T - T_{ref})}{|z_c z_a|} \right) \quad (23)$$

One of the most important features of Meissner's generalized correlation is that with only one data point for γ_{\pm} at a particular electrolyte concentration, extrapolation (or interpolation) to any other concentration value can be made. This is sometimes valid for compositions that even exceed the saturation value (solubility) of that salt, which is a valuable feature for multicomponent systems [21]. However, one of the downsides of the Meissner model is its limited capability for extrapolation to temperatures higher than the base temperature of 298 K. This is a direct result of the fact that only one adjustable parameter is employed. The model is also limited in accurately capturing the effects of other cosolvents. Nonetheless, when considering water desalination as the intended use, these constraints do not pose significant limitations.

2.5. Numerical Solution Strategy

For a given aqueous phase with a known electrolyte concentration, (γ_{\pm}^s) is calculated using the selected liquid phase electrolyte model for the mean ionic activity coefficient, i.e., the DH and Meissner models. Together with the known charge density of the IEM (q) as an input parameter, Equation (11) or Equation (12) are solved iteratively for C_A^m , and hence Equation (5) is used to solve for E_{Don} . The concentration of the cation inside the membrane (C_C^m) is obtained directly from Equation (8). The flow chart for the numerical solution employed in this work and implemented using Excel spreadsheets (Microsoft® Excel® 2016) is shown in Figure 1.

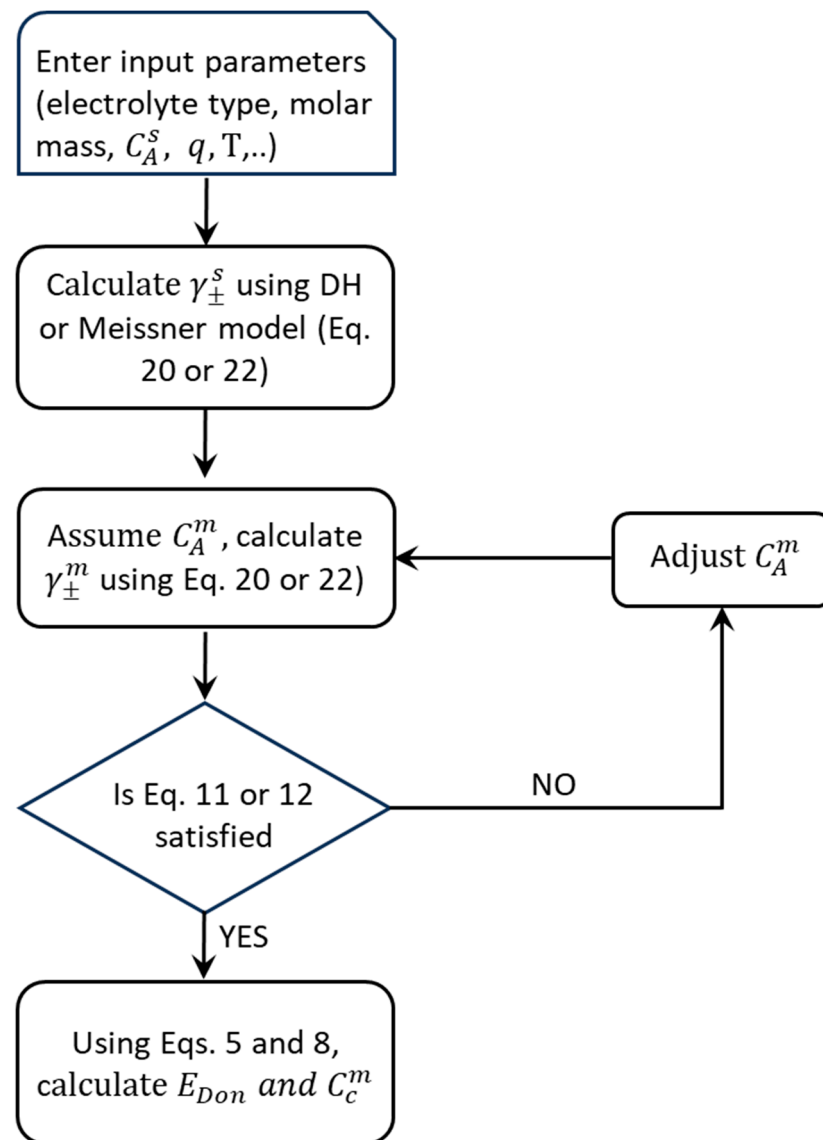


Figure 1. The flow chart implemented in calculating the Donnan potential in the NaCl-IEM system.

3. Results and Discussion

3.1. Model Verification

Verifying Donnan's potential associated with IEMs in a certain electrolyte system is highly prioritized in developing novel perm-selective membranes. However, due to the lack of appropriate interfacial experimental techniques, direct measurement of Donnan's potential is complicated and difficult to attain. Most recently, Gokturk et al. [14] developed an experimental methodology for directly measuring Donnan potential for commercial IEMs equilibrated with electrolyte solutions and presented experimental results for the cases of NaCl and MgCl₂ aqueous salt solutions. Their measurements are based on the binding energy shift in membrane-related core levels detected by a tender ambient pressure X-ray. The authors compared their experimental measurements with model predictions. They applied Manning's counter-ion condensation theory to predict the ion activity coefficients inside a commercial IEM and the Pitzer model to calculate the ion activity coefficients in the external salt solutions [24,25]. This approach requires the input of basic membrane properties, but no adjustable parameters are needed. Reasonable agreement was observed between their experimental measurements and model predictions.

In this work, the Meissner model, a generalized corresponding state activity coefficient model that proved very reliable as a predictive model for treating highly concentrated

solutions, is used to predict activity coefficients. Figure 2 compares the experimental measurements of Gokturk et al. [14] for both NaCl and MgCl₂ with model predictions using the Meissner model. Reasonable agreement is observed, which verifies to some extent both the applicability of the experimental approach of Gokturk and the suitability of the Meissner model for handling highly concentrated electrolyte aqueous solutions. Model prediction for both electrolytes overestimates Donnan's potential. In view of Equation (5), this is equivalent to saying that the Meissner model either underestimates the ionic activity inside the membrane relative to the actual value or overestimates the ionic activity in the external aqueous feed solution. However, the model was proven to give excellent predictions for aqueous phases of electrolytes up to and even exceeding a molality of six [21]. The predicted concentration of the ion inside the membrane is probably underestimated by the model, which leads to lower than actual ionic activity inside the membrane. It is also observed that the Donnan potential is lower for higher-valence counter-ions (e.g., Mg²⁺), leading to reduced co-ion exclusion, which is in agreement with Gokturk et al. [14].

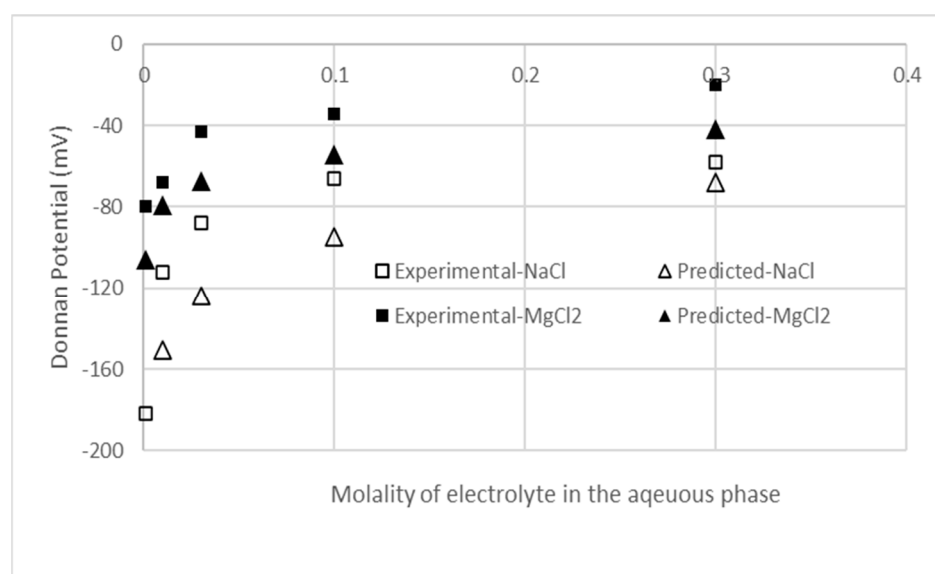


Figure 2. Comparison between experimental Donnan potential in the NaCl–IEM system and Meissner model prediction.

3.2. Effects of Osmotic Pressure, Ionic Adsorption, and Ionic Pairing on Donnan Potential

As mentioned in Section 2.2, researchers have reported that coupling between ion concentrations and the osmotic pressure (π) can give rise to a membrane potential that consists of not only the classical Donnan potential term but also an additional term due to the osmotic pressure [20,21]. According to these investigators, this coupling can lead to the existence of a membrane potential even when the impermeable species are not charged [21]. For a (1–1) electrolyte like NaCl, Equations (14) and (17) show that the osmotic pressure effect is given by the dimensionless function $f(\pi)$, which is simply the ratio of the activity of water in the feed and the membrane phases (a_{water}^s/a_{water}^m) raised to the exponent ($\bar{V}_{solute}/2\bar{V}_{water}$). The activity of water in each phase is a function of the water mole fraction in that phase, which in turn depends on the equilibrium composition of the electrolyte. Since the water mole fraction in both phases, the swelled membrane phase (m) and the feed phase (s), is not drastically different from each other, the activity ratio is not expected to significantly differ from unity. Our computation shows that for an extreme case of a membrane fixed charge density of 15 eq/L, x_w^s (the feed phase mole fraction of water) is less than 5% different from x_w^m (the membrane phase mole fraction of water). This implies that, within the parameters examined in this study, the impact of osmotic pressure is expected to be negligible. To verify this, the Donnan potential was recalculated with the osmotic pressure taken into account for two extreme cases of the membrane fixed charge density,

i.e., 1 eq/L and 15 eq/L. The difference between Donnan potential corrected for osmotic pressure and Donnan potential without osmotic pressure correction is shown in Figure 3. The required partial molar volume of water \bar{V}_{water} is taken as $18 \text{ cm}^3/\text{mol}$, and the partial molar volume of the (NaCl) electrolyte \bar{V}_{solute} is calculated using the experimental data recently reported by Khons et al. [26]. No effect of the osmotic pressure is observed for a fixed charge density of 1 eq/L. Even for the extreme case of 15 eq/L, the maximum difference in Donnan potential is 1 mV, less than 5% of the conventional Donnan potential. The observed maximum in Figure 3 for the case of 15 eq/L is a result of the opposing values of the two terms appearing in Equation (14), i.e., the activity term and the osmotic pressure term.

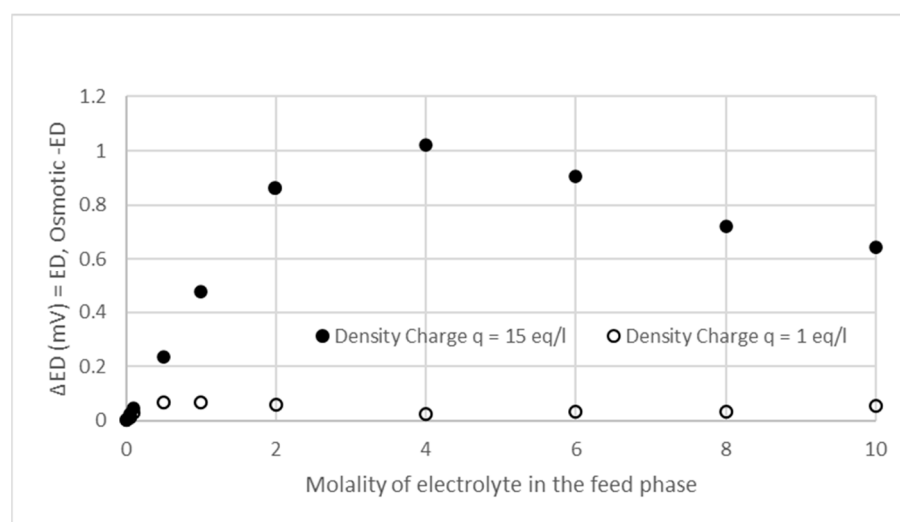


Figure 3. Effect of electrolyte molality and membrane fixed charge density on the difference in Donnan potential with and without osmotic pressure correction in the NaCl–IEM system.

The effects of adsorbed ions on the Donnan potential, which develops at the IEM interphase, are particularly interesting in ion exchange membranes [27,28]. It is worth mentioning that ion adsorption on localized membrane sites gives rise to a non-ideal or modified Donnan phenomenon. This phenomenon arises because of the electrostatic interaction between adsorbed ions and the dependence of the concentration of adsorbed ions on external solution conditions such as electrolyte concentration and pH [29]. The modified Donnan potential is usually computed by augmenting an adsorption isotherm that incorporates the interaction between adsorbed ions into the Donnan formalism [30]. Such theoretical studies are of special importance as they delineate the conditions under which interaction between adsorbed ions is important enough to be considered. The interaction of water molecules with charged surfaces and the influence of the surface on the structure of the extended hydrogen bond network is a subject of ongoing extensive studies [31,32].

Another phenomenon that has a similar effect on Donnan equilibrium is that of the counterion-membrane-fixed ion pairing in charged membranes with low dielectric constant regions. Here, the ideal Donnan equilibrium is extended to account for the ion pairing effect, such as the Fuoss approach for contact ion pairs in electrolyte solutions with a correction term for the entropy change in the counter-ion undergoing ion pairing [33].

3.3. Effects of Membrane Fixed Charge Density and Electrolyte Concentration

In our analysis, the effects of osmotic pressure, ion adsorption, and ion pairing are not included. The osmotic pressure shown above does not have a significant effect under the conditions of this study. Adsorption and ion pairing interactions with Donnan potential could be an interesting topic that can be addressed in a separate study; including them in this manuscript could potentially lead to a substantial increase in its overall length. It is worth mentioning that the saturation solubility of NaCl in water at 298 K is about 6 moles

of salt per kg of water and that it is not sensitive to moderate temperature changes [34]. Despite this, it is not uncommon to find in the technical literature research studies on NaCl solutions with compositions exceeding the saturation solubility [35]. Such supersaturated aqueous salt solutions, where solutes in excess of the expected equilibrium solubility are encountered, are a very well-known phenomenon, especially in the crystallization-related technical literature. However, such systems are thermodynamically metastable [19]. Another phenomenon that can contribute to supersaturation is ion association. In a simulation study by Soniat et al. [36], it was found that for NaCl, NaI, and KCl, larger clusters are present but with a small amount of pairing.

The effect of the IEM fixed charge density (q) on the generated Donnan potential, using the classical DH and Meissner models, is shown in Figure 4. The results in this figure reveal excellent agreement between the DH and Meissner models for electrolyte concentrations up to a molality of 0.1 (approximately 6000 ppm). Beyond this concentration, however, the DH model overestimates the predicted (absolute) Donnan potential relative to the Meissner model. The difference between the predictions of the two models grows with the electrolyte feed concentration. The overestimate of the predicted Donnan potential by the DH model is attributed to the basic assumptions inherent in the DH model. Also, at higher feed concentrations of the electrolyte, the mismatch between the two models grows with the level of the IEM fixed charge. For example, at an electrolyte concentration of 0.2 M (11,688 ppm), the DH model overestimates Donnan potential by approximately the same amount of 5 mV relative to the Meissner model for the three levels of fixed charge density investigated in this study, i.e., 1, 2, and 5 equivalent/L. However, the corresponding overestimates of Donnan potential for an electrolyte concentration of 5 M (292,200 ppm) are 13, 29, and 50 mV for the fixed charge densities of 1, 2, and 5 equivalent/L, respectively. This can result from a higher degree of deviation from ideal solution behavior (i.e., the equal activity coefficient of the ions inside the membrane and in the aqueous feed phase), an inherent assumption in the DH model. Figure 4 also reveals that a higher (absolute) Donnan potential is obtained by a higher IEM fixed charge. This is expected given the higher exclusions of co-ions at the high IEM fixed charge [12].

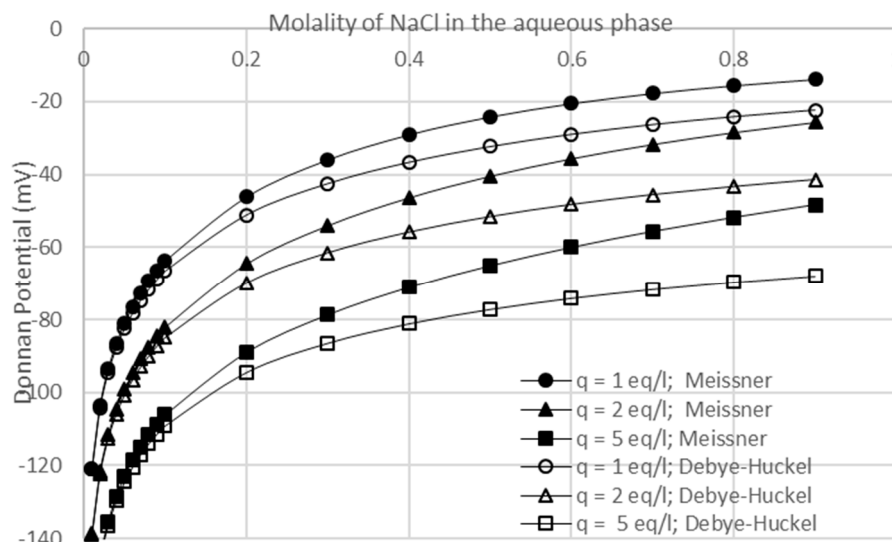


Figure 4. Predicted Donnan potential for the NaCl–IEM system at 298 K for three levels of the fixed charge.

Figure 5 presents the effect of the electrolyte concentration in the feed on the co-ion concentration inside the IEM for three levels of the fixed charge concentration as predicted by the DH and the Meissner model. The two models agree in their predictions for electrolyte feed concentrations up to 5000 ppm. However, the two models seriously disagree in their

predictions beyond that concentration. The DH model predicts higher exclusion, i.e., a lower concentration of the co-ion inside the IEM.

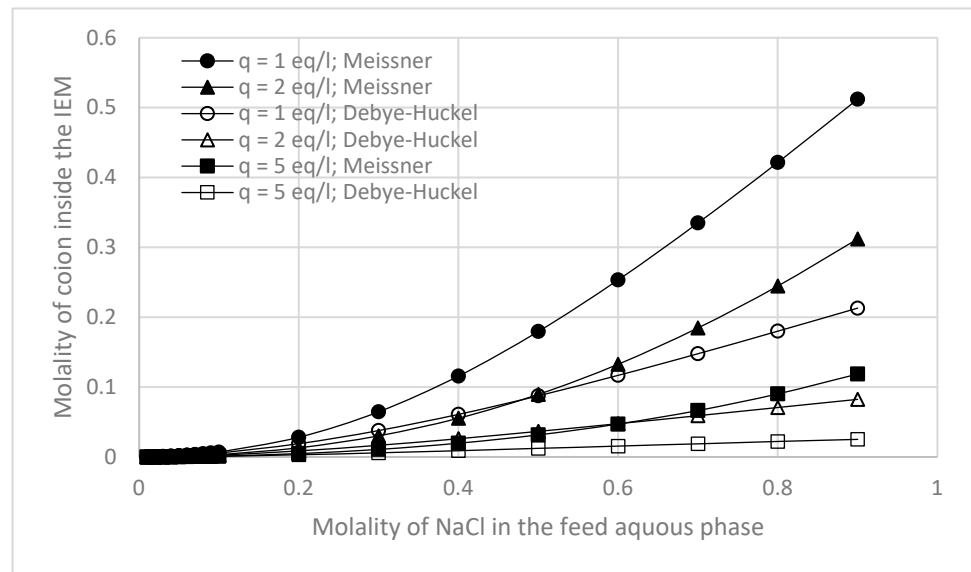


Figure 5. Predicted co-ion concentration inside the IEM at 298 K for three levels of the fixed charge.

Figure 6 shows the effect of the IEM fixed charge density on the membrane anion-to-cation concentration ratio ($C_{Cl^-}^m / C_{Na^+}^m$), as predicted by both the DH and Meissner models. This ratio is indicative of the IEM perm-selectivity. The DH model agreement with the Meissner model breaks after approximately an electrolyte concentration of 1 M. The DH model predicts a total exclusion (zero concentration) of the co-ion for the fixed charge of 5 equivalents per liter and a minimum exclusion (maximum concentration) at a bulk electrolyte concentration of 3 M for the case of a fixed charge of 1 equivalent per liter. On the other hand, the Meissner model correctly predicts the 100% asymptotic limiting value of ($C_{Cl^-}^m / C_{Na^+}^m$) as the bulk concentration of the electrolyte increases.

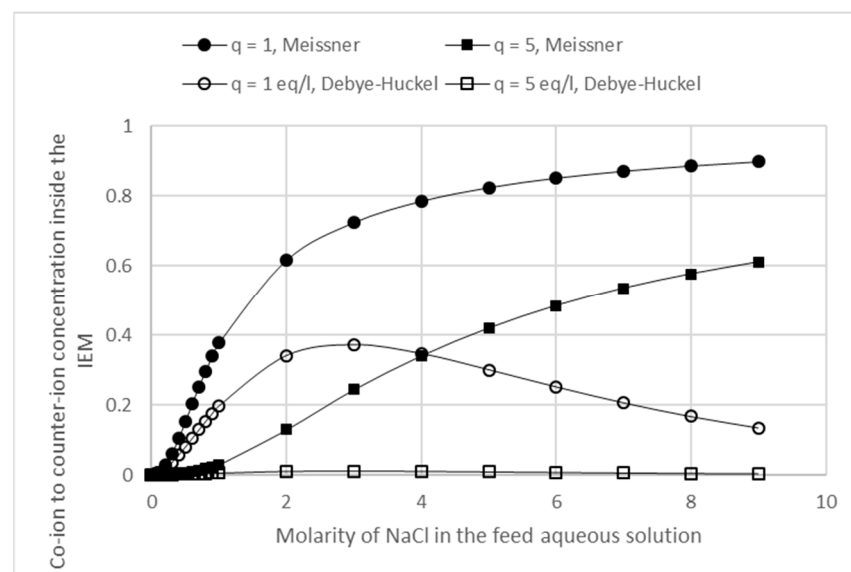


Figure 6. Effect of the IEM fixed charge on ($C_{Cl^-}^m / C_{Na^+}^m$) as predicted by the DH and Meissner models.

4. Conclusions

Ion exchange membranes play a vital role in electrically driven membrane processes. The effect of the ionic strength of the treated feed solutions and the fixed charge density of the ion exchange membrane on the associated Donnan potential is investigated using two predictive models, i.e., the Debye–Huckel and the Meissner models. The latter model is verified using one set of experimental data that was recently reported in the literature. The high concentration of the feed aqueous phase deteriorates membrane selectivity. A high fixed charge density is required to counterbalance such deterioration in selectivity. The DH model can be safely used to predict the equilibrium Donnan potential for feed phase composition up to 0.1 M. Beyond this threshold composition, the DH model significantly overestimates the predicted (absolute) Donnan potential compared to the predictions by the Meissner model. The osmotic pressure effect on Donnan potential, which results from the difference in co-ion concentration between the membrane phase and the feed phase, is shown not to be significant.

Author Contributions: Conceptualization, N.A.D.; Formal analysis, B.A.K.A.-S., G.A.H. and N.A.D.; Writing—review & editing, N.A.D. All authors have read and agreed to the published version of the manuscript.

Funding: The work in this paper was supported, in part, by the Open Access Program from the American University of Sharjah.

Data Availability Statement: An example of the Excel spreadsheets which were used to generate the results in this paper is available upon request.

Conflicts of Interest: The authors declare no conflict of interest.

Disclaimer: This paper represents the opinions of the author(s) and does not mean to represent the position or opinions of the American University of Sharjah.

References

1. Lee, S.B.; Kim, J.H.; Lee, H.B.; Lee, J.W. Advances in microfluidic membrane emulsification for water desalination. *J. Membr. Sci.* **2020**, *610*, 118258.
2. Wang, S.; Zhang, Q.; Chen, T.; Ma, Y. Microfluidic electrochemical desalination: Principles, applications, and perspectives. *J. Membr. Sci.* **2021**, *635*, 119512.
3. Lin, Y.; Cheng, J. Recent advances in microfluidic-based electrodialysis for desalination. *J. Mater. Chem. A* **2021**, *9*, 159–180.
4. Al-Amshawee, S.; Yunus, M.Y.; Azoddein, A.M.; Hassell, D.G.; Dakhil, I.H.; Abu Hasan, H. Electrodialysis desalination for water and wastewater: A review. *Chem. Eng. J.* **2020**, *380*, 122231. [[CrossRef](#)]
5. Ma, J.J. Research progress on separation and purification of whey protein based on membrane technology. *Chem. Ind. Eng. Prog.* **2022**, *41*, 2826–2838.
6. Liang, T.; Lu, H.; Ma, J.; Sun, L.; Wang, J. Progress on membrane technology for separating bioactive peptides. *J. Food Eng.* **2023**, *340*, 111321. [[CrossRef](#)]
7. Nayak, S.K.; Dutta, K.; Gohil, J.M. (Eds.) *Advancements in Polymer-Based Membranes for Water Remediation*; Elsevier Inc.: Amsterdam, The Netherlands, 2022.
8. Liu, Y.; Wu, X.; Dai, L.; Wu, X.; Ding, J.; Chen, R.; Ding, R.; Liu, J.; Van der Bruggen, B. Recovery of nickel in the form of Ni(OH)₂ from plating wastewater containing Ni-EDTA using bipolar membrane electrodialysis. *Chemosphere* **2023**, *310*, 136822. [[CrossRef](#)]
9. Kumar, P.S.; Varsha, M.; Rathi, B.S.; Rangasamy, G. Electrodeionization: Principle, techniques and factors influencing its performance. *Environ. Res.* **2023**, *216*, 114756. [[CrossRef](#)]
10. Ba, X.; Chen, J.; Wang, X.; Wang, J.; Jiang, B. An integrated electrolysis-microfiltration-ion exchange closed-loop system for effective water softening without chemicals input and spent regenerant discharge. *Desalination* **2023**, *553*, 116481. [[CrossRef](#)]
11. Chen, W.; Shen, H.; Gong, Y.; Li, P.; Cheng, C. Anion exchange membranes with efficient acid recovery obtained by quaternized poly epichlorohydrin and polyvinyl alcohol during diffusion dialysis. *J. Membr. Sci.* **2023**, *674*, 121514. [[CrossRef](#)]
12. Tanaka, Y. *Ion Exchange Membranes Fundamentals and Applications*, 2nd ed.; Elsevier: Amsterdam, The Netherlands, 2015.
13. Mulder, M. *Basic Principles of Membrane Technology*, 2nd ed.; Kluwer Academic Publishers: Amsterdam, The Netherlands, 1996.
14. Gokturk, P.A.; Sujanani, R.; Qian, J.; Wang, Y.; Katz, L.E.; Freeman, B.D.; Crumlin, E.J. The Donnan potential revealed. *Nat. Commun.* **2022**, *13*, 5880. [[CrossRef](#)]
15. Higa, M.; Taniokaa, A.; Kirab, A. A novel measurement method of Donnan potential at an interface between a charged membrane and mixed salt solution. *J. Membr. Sci.* **1998**, *140*, 213–220. [[CrossRef](#)]

16. Higa, M.; Kira, A.; Tanioka, A.; Miyasaka, K. Ionic partition equilibrium in a charged membrane immersed in a mixed ionic solution. *J. Chem. Soc. Faraday Trans.* **1993**, *89*, 3433–3435. [[CrossRef](#)]
17. Higa, M.; Kira, A. Theory and simulation of ion transport in nonstationary states against concentration gradients across ion-exchange membranes. *J. Phys. Chem.* **1992**, *96*, 9518–9523. [[CrossRef](#)]
18. Sonin, A.A.; Grossman, G. Ion transport through layered ion exchange membranes. *J. Phys. Chem.* **1972**, *76*, 3996–4006. [[CrossRef](#)]
19. Tester, J.W.; Model, M. *Thermodynamics and Its Applications*, 3rd ed.; Prectice Hall PTR: Hoboken, NJ, USA, 1997.
20. Scotto, J.; Florit, M.L.; Posadas, D. The effect of membrane equilibrium on the behavior of electrochemically active polymers. *J. Electroanal. Chem.* **2016**, *774*, 42–50. [[CrossRef](#)]
21. Chen, G. *Donnan Equilibrium Revisited: Coupling between Ion Concentrations, Osmotic Pressure, and Donnan Potential*; World Scientific Pub Co Pte Ltd.: Singapore, 2022; Volume 7, Available online: <https://hdl.handle.net/1721.1/150833> (accessed on 22 May 2023).
22. McQuarrie, D.A. *Statistical Mechanics*; Harper and Row: New York, NY, USA, 1976.
23. Meissner, H.P.; Tester, J.W. Activity coefficients of strong electrolytes in aqueous solutions. *Ind. Eng. Chem. Proc. Des. Dev.* **1972**, *11*, 128–133. [[CrossRef](#)]
24. Kitto, D.; Kamcev, J. Manning condensation in ion exchange membranes: A review on ion partitioning and diffusion models. *J. Polym. Sci.* **2022**, *60*, 2929–2973. [[CrossRef](#)]
25. Pitzer, K.S. Thermodynamics of electrolytes. I. Theoretical basis and general equations. *J. Phys. Chem.* **1973**, *77*, 268–277. [[CrossRef](#)]
26. Kohns, M.; Horsch, M.; Hasse, H. Partial molar volume of NaCl and CsCl in mixtures of water and methanol by experiment and molecular simulation. *Fluid Phase Equilibria* **2018**, *458*, 30–39. [[CrossRef](#)]
27. Mafe, S.; Manzanares, J.A.; Reiss, H. Donnan phenomena in membranes with charge due to ion adsorption. Effects of the interaction between adsorbed charged groups. *J. Chem. Phys.* **1993**, *98*, 2325–2331. [[CrossRef](#)]
28. Takagi, R.; Nakagaki, M. Theoretical study of the effect of ion adsorption on membrane potential and its application to collodion membranes. *J. Membrane Sci.* **1990**, *53*, 19–35. [[CrossRef](#)]
29. Laksminarayanaiah, N. *Transport Phenomena in Membranes*; Academic Press: New York, NY, USA, 1969.
30. Manzanares, J.A.; Mafe, S.; Bisquert, J. Electric Double Layer at the Membrane/Solution Interface: Distribution of Electric Potential and Estimation of the Charge Stored. *Phys. Chem.* **1992**, *96*, 538–544. [[CrossRef](#)]
31. Dewan, S.; Carnevale, V.; Bankura, A.; Eftekhari-Bafrooei, A.; Fiorin, G.; Klein, M.L.; Borguet, E. Structure of Water at Charged Interfaces: A Molecular Dynamics Study. *Langmuir* **2014**, *30*, 8056–8065. [[CrossRef](#)]
32. Gonella, G.; Backus, E.H.G.; Nagata, Y.; Bonthuis, D.J.; Loche, P.; Schlaich, A.; Netz, R.R.; Kühnle, A.; McCrum, I.T.; Koper, M.T.M.; et al. Water at charged interfaces. *Nat. Rev. Chem.* **2021**, *5*, 466–485. [[CrossRef](#)]
33. Mafe, S.; Ramirez, P.; Tanioka, A.; Pellicer, J. Model for Counterion-Membrane-Fixed Ion Pairing and Donnan Equilibrium in Charged Membranes. *J. Phys. Chem. B* **1997**, *101*, 1851–1856. [[CrossRef](#)]
34. Sawamura, S.; Egoshi, N.; Setoguchi, Y.; Matsuo, H. Solubility of sodium chloride in water under high pressure. *Fluid Phase Equilibria* **2007**, *254*, 158–162. [[CrossRef](#)]
35. Jiang, H.; Debenedetti, P.G.; Panagiotopoulos, A.Z. Nucleation in aqueous NaCl solutions shifts from 1-step to 2-step mechanism on crossing the spinodal. *J. Chem. Phys.* **2019**, *150*, 124502. [[CrossRef](#)]
36. Soniat, M.; Pool, G.; Franklin, L.; Rick, S.W. Ion association in aqueous solution. *Fluid Phase Equilibria* **2016**, *407*, 31–38. [[CrossRef](#)]

Disclaimer/Publisher’s Note: The statements, opinions and data contained in all publications are solely those of the individual author(s) and contributor(s) and not of MDPI and/or the editor(s). MDPI and/or the editor(s) disclaim responsibility for any injury to people or property resulting from any ideas, methods, instructions or products referred to in the content.